OPTOELECTRONICS AND ADVANCED MATERIALS – RAPID COMMUNICATIONS Vol. 4, No. 5, May 2010, p. 630 - 636

Preparation and characterization of a micro-porous polymer electrolyte based on polymeric ionic liquid for dye-sensitized solar cell

YANG YAN, TAO JIE*, JIN XIN, QIN QI
College of Material Science and Technology, Nanjing University of Aeronautics and Astronautics, Nanjing 210016, P.R. China

Poly (1-vinyl-3-propylimidazolium) iodide (P(ViPrIm$^+$I$^-$)) was synthesized in an environmentally friendly way in order to develop a micro-porous polymer electrolyte for quasi-solid-state dye sensitized solar cells. The samples were characterized by Fourier Transform Infrared Spectroscopy, differential scanning calorimeter and Scanning Electron Microscope respectively. Moreover, the ionic conductivity of the electrolytes was measured by electrochemical workstation. The results indicated that the incorporation of P(ViPrIm$^+$I$^-$) component into the polymer matrix changed significantly the morphology and improved the electrochemical behavior of the gel polymer electrolyte. The P(ViPrIm$^+$I$^-$) can act as not only the polymer matrix but also the source of iodide. A dye-sensitized solar cell employing gel polymer electrolyte yielded an open-circuit voltage of 0.694 V, short-circuit current of 12.752 mAcm^{-2} and the conversion efficiency of 5.66% at 1 sun illumination.

(Received April 28, 2010; accepted May 20, 2010)

Keywords: Polymeric ionic liquid, Dye-sensitized solar cell, Polymer gel electrolyte, Ionic conductivity, Photovoltaic performance

1. Introduction

Dye-sensitized solar cells (DSSCs) are becoming a promising alternative to classical photovoltaic devices based on inorganic semiconductor technology because of their possible low production cost and the expected high energy conversion efficiency [1]. DSSCs with liquid electrolyte prepared have reached the efficiency of as high as 11.04% [2]. However, the main problem is that the liquid electrolytes limit device stability because of easy evaporation and leakage. For improving the long-term stability, many attempts have been made to substitute the volatile liquid electrolytes with quasi-solid-state electrolytes (e.g. polymer gel [3], low-molecular-weight gel [4], or ureasil/sulfolane gel [5]) or solid state electrolytes (e.g. p-type semiconductors [6], organic hole-transport materials [7], solid polymer electrolytes [8], and plastic crystal electrolytes [9]).Room temperature ionic liquids with the attractive properties of chemical and thermal stability, non-volatility and high ionic conductivity in room temperature were studied extensively for the electrochemical device applications. Various investigations have been carried out to develop the ionic liquid electrolytes as the promising candidate for DSSCs [10–14]. Furthermore, there are many interests in preparing the quasi-solid state electrolytes by solidifying the ionic liquid electrolytes with small molecular organogels [15], polymers [16] or nanoparticles [17].

Polymeric ionic liquid (PIL) is a functional polymer presenting some of the characteristics of ionic liquid. It has showed to be excellent matrices to design polymer electrolytes [18–21]. Bo Yu, et al. [22] prepared poly ionic liquid 1-ethyl 3-(2-methacryloyloxy ethyl) imidazolium iodide (PEMEImI) as a single-ion conductor. The complex based on PAN-PEMEImI-I_2-EC/PC formed gel polymer electrolyte. The gel polymer electrolyte had good ionic conductors with high ionic conductivity of above 1×10^{-3} S cm^{-1} in optimal proportion of the components at room temperature. Eneko Azaceta, et al. [23] reported a series of polymer electrolytes formulated as mixtures of the ionic liquid 1-methyl-3-propylimidazolium iodide and the poly(1-vinyl-3-alkylimidazolium) iodide polymers. Gel electrolytes was obtained by adding poly(1-vinyl-3-propylimidazolium) iodide into a typical acetonitrile electrolyte and tested in DSSCs. The results showed that DSSCs employing the gel polymer electrolyte yielded a maximum light-to-electricity conversion efficiency of 3.73%.

The methods mentioned above were direct dissolution of polymeric ionic liquid in the electrolyte solution. The softening of the polymer makes the cell assembly difficult and increases the incidence of short-circuiting between the electrodes. In this study, a new polymer gel electrolyte (GPE) is fabricated by soaking a porous polymer membrane based on poly (vinylidene fluoride) -poly(1-vinyl-3-propylimidazolium) iodide hybrid in the conventional organic liquid electrolyte. GPE membrane with porous structure possesses numerous advantages such as a free-standing framework, high ionic conductivity and ease of cell fabrication. Pores closely interconnected to each other make the ion transportation in polymer membrane similar to the behavior in liquid electrolytes so that the porous structure can improve the ionic conductivity of GPE membranes. Moreover, it is advantageous to hold liquid electrolytes and improve the contact property between electrolyte and electrode, resulting in an enhancement of the photovoltaic performance of the DSSCs [24].

Unlike other usual polymer matrixes, we designed polymeric ionic liquid with iodide as an anionic counterpart. Poly(1-vinyl-3-propylimidazolium) iodide is expected to serve as a new class of iodide ion source. It can enhance the stability of the electrolytes and possibly be advantageous in transport of anionic species in the cell. Systematic studies were performed to understand the influence of these polymeric ionic liquids on the performance of DSSCs when they were used as a component of gel polymer electrolytes.

2. Experimental

2.1 Synthesis of poly(1-vinyl-3-propylimidazolium) iodide

Teflon-lined, stainless autoclaves were employed for the synthesis of 1-vinyl-3-propylimidazolium iodine under solvent-free conditions [25]. It was an improved and environmentally friendly preparation. The mixture of 1-vinylimidazolium (50.0 mmol) and n-propyl iodide (52.5 mmol) was placed in a 50 mL Teflonlined, stainless steel autoclave, and then was heated in an oven at 100℃ for 4 h. The resulting white-yellowish liquid was allowed to cool down to room temperature to become solid. The solid product was washed several times with ethyl ether, then dried in a vacuum oven at 80℃ for 24h.

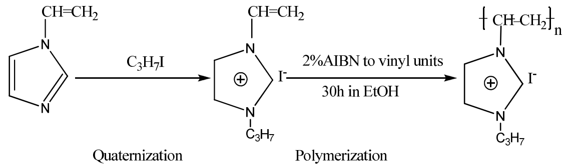

Scheme 1. Synthesis of poly(1-vinyl-3-propylimidazolium) iodide.

Previously synthesized monomers were diluted in ethanol in a 100-mL round-bottom flask. Then 2 wt.% 2, 2'-azobis (isobutyronitrile) (AIBN) as radical initiator was added to the mixture. The solution was heated for 30 h at 85 ◦C under Ar_2 atmosphere. The obtained white-yellowish solid precipitate was washed several times with chloroform and dried in a vacuum oven until constant weight. ^{1}HNMR (500MHz, $CDCl_3$)δ:1.02-1.04(t,3H), 2.00-2.06(m,2H), 4.41-4.44(t,2H), 5.45-5.46(m, 1H), 6.01-6.03(m, 1H), 7.43-7.46(m, 1H), 7.66(s, 1H), 7.84(s, 1H), 10.54(s, 1H).

2.2 Preparation of polymer electrolyte

The dry porous polymer membrane composed of poly(vinylidene fluoride) (PVDF, SOLEF 1015) and poly(1-vinyl-3-propylimidazolium) iodide (P(ViPrIm$^+$I$^-$)) was synthesized by the phase inversion process. The dried polymer powders of PVDF and P(ViPrIm$^+$I$^-$) were dissolved in N, N-dimethylformamide (DMF). The weight ratios of PVDF/ P(ViPrIm$^+$I$^-$) polymer mixtures were 9/1 , 8/2, 7/3, 6/4, 5/5, and 6/4 respectively. An amount of propanetriol as nonsolvent was then added under continuous stirring at 60 for 12h to form homogeneous hybrid. The resulting viscous mixture spread on a glass substrate was heated to 80 for 24 h to remove solvent and nonsolvent.

The formed films were immersed in ethanol to extract residual propanetriol. Finally the dried polymer membranes were soaked in liquid electrolyte (0.5mol/l NaI, 0.05 mol/l I_2, 0.1 mol/l 4-tert-butylpyrdine in the binary organic solvents mixture propylene carbonate and ethylene carbonate with 4:6 (w/w) for 12 h to obtain the desired gel polymer electrolytes.

2.3 Preparation of TiO_2 photoanode

Self-aligned highly ordered TiO_2 nanotube arrays were fabricated by potentiostatic anodic oxidation in a two-electrode electrochemical cell [26]. The separation distance between the electrodes was 4 cm. The voltage applied between Ti-foil anode and Pt cathode was 20 V at room temperature. The electrolyte used was ethylene glycol solution with an addition of H_2O (1 vol.%) and NH_4F (0.25 wt.%). All solutions were prepared from reagent grade chemicals. Prior to anodization, all the Ti-foil samples were cleaned with acetone and ethanol, chemically polished to a mirror image by the polishing solution, then rinsed with distilled water and dried in nitrogen stream. Only one face of the Ti-foil was exposed to the electrolyte during anodization by tape-masking the other face. TiO_2 nanotube arrays having lengths up to 20 μm were grown in vertical direction to the underlying Ti-foil with an exposed area of 0.25cm^2.

The as-prepared nanotube Ti-foil was thoroughly washed with distilled water. Then they were crystallized into anatase phase after annealing at 450 °C for 3h in oxygen atmosphere because as-anodized TiO_2 nanotubes were amorphous phase.

2.3 Assemble of dye-sensitized solar cells

The TiO_2 film was immerged in a 0.5mmol ethanol solution of *cis*-[$(dcbH_2)_2Ru(SCN)_2$] (N719; Solalonix) for 24 hours to absorb the dye adequately, the other impurities were washed up with anhydrous ethanol and dried in moisture-free air. After that, a dye-sensitized TiO_2 film was prepared.

A quasi-solid-state dye-sensitized solar cell was assembled by sandwiching a slice of gel polymer electrolyte between a dye sensitized TiO_2 electrode and a platinum counter electrode. The two electrodes were clipped together with clamps. For comparison, a DSSC with conventional liquid electrolyte was also assembled. The active area of the cell was $0.25 cm^2$.

2.4 Measurements

^{1}HNMR was recorded on a 500 MHz spectrometer (BRUKER DRX500) using $CDCl_3$ as solvent. The IR absorption spectra were taken using an attenuated total reflection Fourier transform infrared spectrometer (PerkinElmer1760) over the range from 600 to 4000 cm^{-1}. The morphology of polymer membrane was characterized by scanning electron micrograph (Quanta200, FEI).

The thermal behavior of the samples was studied by means of differential scanning calorimeter (CDR-1) with a scan rate of 10□/min. The melting temperature (T_m) and the heat of fusion (ΔH_f) were determined from the obtained melting endotherms. The crystallinity of the polymer membranes (X_c) was calculated by dividing the measured ΔH_f by the value for perfect PVDF crystal (ΔH^0 = 105 J/g) obtained from the literature [27].

$$X_c = (\Delta H_f / \Delta H^0) \times 100\% \tag{1}$$

The electrolyte uptake was calculated by:

$$\text{Uptake} = (W_i - W_0) / W_0 \times 100\% \tag{2}$$

where W_i and W_0 are the weight of the wet and dry membranes, respectively;

The porosity of membranes was measured by immersing the membranes into *n*-butanol for 1 h. The porosity was calculated using the following equation [28]:

$$\text{Porosity} = (M_b / \rho_b) / [(M_p / \rho_p) + (M_b / \rho_b)] \times 100\% \tag{3}$$

Here, M_p is the weight of membrane, M_b is the weight of absorbed *n*-butanol, ρ_p is the density of the membrane and ρ_b is the density of *n*-butanol, respectively.

The symmetric cell was built to characterize electrochemical properties of electrolyte with a similar design as DSSC by sandwiching the GPE sample between two Pt electrodes (Pt/electrolyte/ Pt).

The electrolyte resistance R_b was measured using CHI660 electrochemical workstation. The ionic conductivity of the GPE was calculated with the equation:

$$\sigma = d / R_b S \tag{4}$$

where d is the thickness of electrolyte and S is the area of electrolyte.

To investigate the diffusion coefficients of I_3^- in the electrolyte, steady-state voltammograms of GPE was performed. The apparent diffusion coefficients of triiodide (D) were calculated according to the equation as follows [29]:

$$D = I_{\text{lim}} d / 2nFC \tag{5}$$

where I_{lim} is limiting current density , n is the electron number per molecule, d is the thickness of gel electrolyte, F is the Faraday constant and C is the bulk concentration of electroactive species.

Photocurrent-voltage characteristics of the DSSCs were obtained by a Keithley model 2400 digital source meter using an Oriel 91192 solar simulator equipped with AM 1.5 filter and intensity of $100 mW/cm^2$.The fill factor and the conversion efficiency(η) of the cell are calculated by the following equations [30]:

$$ff = P_{\max} / I_{sc} V_{oc} = I_{mp} V_{mp} / I_{sc} V_{oc} \tag{6}$$

$$\eta = I_{mp} V_{mp} / P_{in} \times 100\% \tag{7}$$

where I_{sc} is the short-circuit current density(mA cm^{-2}),V_{oc} is the open-circuit voltage(V), Pin is the incident light power. I_{mp} (mA cm^{-2}) and V_{mp}(V) are the current density and voltage in the *I*-*V* curves, respectively, at the point of maximum power output.

3. Results and discussion

3.1 FT-IR spectroscopy

Fig. 1 shows FT-IR spectra of the 1-vinyl-3-propylimidazolium iodide monomers and their polymer. The samples show sharp lines at 2971, 2938, 2876cm^{-1} corresponding to $-CH_3-$ and $-CH_2-$ stretching vibration bands on side-chain of imidazole ring, which confirmed successful quaterzination reaction. No peaks observed at 967, 930, 1650 cm^{-1} in spectra of $P(ViPrIm^+I^-)$ indicates that the C=C stretching vibration of vinylidene groups in unpolymerized $ViPrIm^+I^-$ monmer disappeared via polymerization.

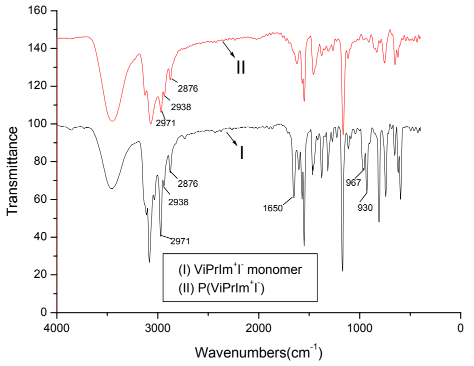

Fig. 1. FT-IR spectra of $ViPrIm^+I^-$ and $P(ViPrIm^+I^-)$.

3.2 DSC measurement

DSC curve of P(ViPrIm$^+$I$^-$) is shown in Fig. 2. The glass transition temperatures (T_g) of P(ViPrIm$^+$I$^-$) is not clearly depicted and no crystallization is observed as expected from amorphous polymer. It is clearly seen that rapid thermal degradation of P(ViPrIm$^+$I$^-$) occurs up to 250 under air atmosphere, which illustrates that the poly ionic liquid possesses excellent thermal stability.

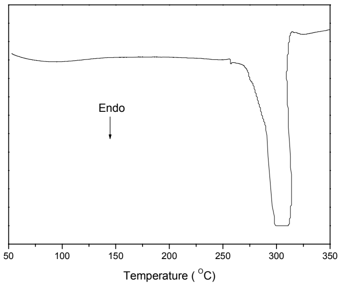

Fig. 2. DSC thermogram of P(ViPrIm$^+$I$^-$).

Fig. 3 shows the DSC thermograms of membranes prepared by the phase inversion process with different PMMA/P(ViPrIm$^+$I$^-$) ratios. The crystallinity data calculated based on the heat of fusion of perfect PVDF crystal (ΔH^0 = 105 J/g) are summarized in Table 1. It can be seen that the melting point (T_m) of PVDF crystals depresses with increasing P(ViPrIm$^+$I$^-$) content. Moreover the incorporation of P(ViPrIm$^+$I$^-$) component into the micro-porous polymer matrix reduces the crystallinity of original polymer matrix.

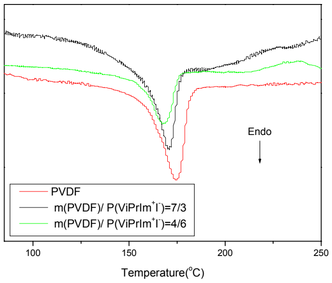

Fig. 3. DSC thermograms of membranes.

Table 1. Melting temperature and the crystallinity of PVDF and PVDF/ P(ViPrIm$^+$I$^-$) membranes.

*m*PVDF/ *m*P(ViPrIm$^+$I$^-$)	T_m (℃)	ΔH_f (J/g)	X_c
10/0	174.39	53.25	0.505
7/3	170.83	46.77	0.445
4/6	167.72	43.70	0.420

3.3 Morphology

The surface of dry polymer membranes with different weight ratios of PVDF/ P(ViPrIm$^+$I$^-$) was observed by SEM, (seeing Fig. 4). All membranes display a surface with a homogeneous porosity. The interior of the membrane has a uniform porous structure as well as the exterior. This indicates that the cellular pores are all open with extensive pore-pore interconnections.

The incorporation of P(ViPrIm$^+$I$^-$) component into the micro-porous polymer matrix changed significantly the morphology. The membrane produced with low content P(ViPrIm$^+$I$^-$) displays regular fibrous porous structure. The size of the pores decrease with the increase of the amount of P(ViPrIm$^+$I$^-$). Meantime the surface shows irregular round-hole voids. As P(ViPrIm$^+$I$^-$) has poor film forming properties, the mechanical property of the polymer membranes decreases with the increase of P(ViPrIm$^+$I$^-$) content. It was found that freestanding film can not form while beyond the amount of P(ViPrIm$^+$I$^-$) content 60%.

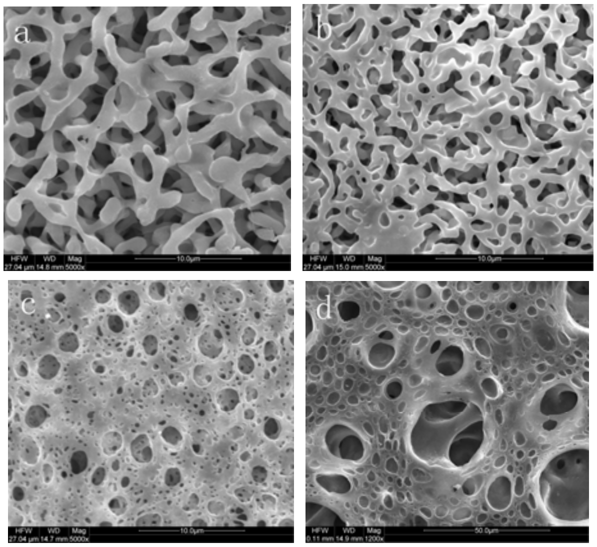

Fig. 4. SEM images of dry polymer membranes: (a) the weight ratio of PVDF/ P(ViPrIm$^+$I$^-$) is 7/3 (b) the weight ratio of PVDF/ P(ViPrIm$^+$I$^-$) is 6/4; (c) the weight ratio of PVDF/ P(ViPrIm$^+$I$^-$) is 5/5; (d) the weight ratio of PVDF/ P(ViPrIm$^+$I$^-$) is 4/6.

3.3. Porosity and electrolyte uptake

Fig. 5 shows the porosity and electrolyte uptake of membranes with different polymer composition. The maximum of the porosity is observed when the weight ratio of PVDF/ P(ViPrIm$^+$I$^-$) polymer is 7/3. The tendency of the electrolyte uptake is similar to that of porosity. The GPEs with 30wt.% P(ViPrIm$^+$I$^-$) and 70 wt.% PVDF has the maximum electrolyte uptake 265.22%. According to Saito and co-workers [31], there are two distinct steps for liquid electrolyte uptake in PVdF-based porous gel polymer membranes. Firstly, the liquid electrolyte occupied some pore spaces of the membrane. Then, those electrolytes in pores penetrated and swelled the polymer chains to form the gel. The electrolyte uptake was found to depend on the porosity of the polymer membranes in this work.

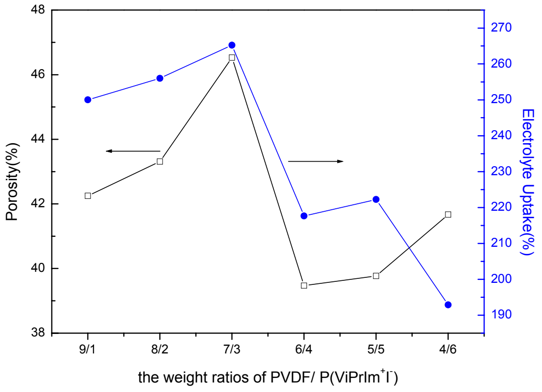

Fig. 5. Porosity and electrolyte uptake of polymer membranes.

3.4 Ionic conductivity and triiodide diffusion coefficients of GPEs

EIS was used to characterize the electrochemical behavior of the gel polymer electrolyte. The ionic conductivity of the GPEs (σ) and the triiodide apparent diffusion coefficient (D) are summarized respectively in Table 2. The presence of P(ViPrIm$^+$I$^-$) can influence the conductivity in different ways. The crystallinity of the membrane is reduced with increasing P(ViPrIm$^+$I$^-$) content as confirmed by DSC analysis, which improves the conductivity of GPEs. But meanwhile, the porosity of the membrane decreases with increasing P(ViPrIm$^+$I$^-$) content, leading to the drop of the conductivity of GPEs. As a result the gel polymer electrolyte shows the highest σ and D when the weight ratio of PVDF/ P(ViPrIm$^+$I$^-$) polymer is 7/3 and then decreased. The greatest value σ and D obtained is 3.93×10^{-3} and 1.884×10^{-6}. It is noteworthy that the GPE with the weight ratio of 4/6 shows favorable apparent diffusion coefficient of triiodide in spite of poor ionic conductivity. It can be assumed that P(ViPrIm$^+$I$^-$) provide more I_3^- as the source of redox species when iodine is added.

Table 2. The ionic conductivity (σ) and the apparent diffusion coefficient of triiodide (D) of QSPE.

mPVDF/mP(ViPrIm$^+$I$^-$)	9 / 1	8 / 2	7 / 3	6 / 4	5 / 5	4 / 6
σ/ S cm^{-1}	5.272×10^{-4}	8.210×10^{-4}	3.93×10^{-3}	1.760×10^{-3}	6.214×10^{-4}	4.260×10^{-4}
D / cm^2 s^{-1}	6.950×10^{-7}	8.347×10^{-7}	1.884×10^{-6}	1.556×10^{-6}	3.086×10^{-7}	1.083×10^{-6}

3.5 Photovoltaic performance

The photocurrent performances for dye sensitized solar cell with different electrolytes (A to F) were tested. The I–V curves are shown in Fig. 6 and cell parameters corresponding to these DSSCs are summarized in Table 3.

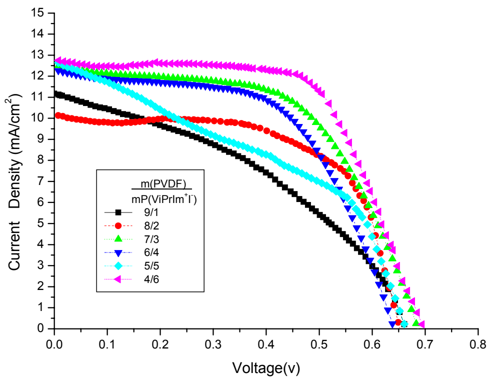

Fig. 6. I–V curves of DSSCs fabricated of various GPEs at 1 sun illumination.

Table 3. Photovoltaic performance of dye sensitized solar cell.

	V_{oc} /V	I_{sc} /mA cm^{-2}	ff	η
Cell A	0.661	11.170	0.403	2.98
Cell B	0.649	10.130	0.627	4.13
Cell C	0.683	12.503	0.572	4.88
Cell D	0.638	12.267	0.572	4.47
Cell E	0.661	12.641	0.419	3.50
Cell F	0.694	12.752	0.639	5.66

The quasi-solid polymer electrolyte used in Cell A is PVDF/ P(ViPrIm$^+$I$^-$) (9:1 m/m);
in Cell B is PVDF/ P(ViPrIm$^+$I$^-$) (8:2 m/m);
in Cell C is PVDF/ P(ViPrIm$^+$I$^-$) (7:3 m/m);
in Cell D is PVDF/ P(ViPrIm$^+$I$^-$) (6:4 m/m);
in Cell E is PVDF/ P(ViPrIm$^+$I$^-$) (5:5 m/m);
in Cell F is PVDF/ P(ViPrIm$^+$I$^-$) (4:6 m/m);

The GPE based on high content PVDF polymer membrane showed poor photovoltaic performance. The addition of P(ViPrIm$^+$I$^-$) brought a significant improvement of the cell performance. According to Saito et al. [32], the porosity, one of the important parameters of porous polymer membranes, can dominate the conduction properties of the carriers. The cell employing GPE of PVDF/P(ViPrIm$^+$I$^-$) (7:3 m/m) showed preferable photovoltaic performance owing to higher the porosity of the micro-porous network.

To our surprise the cell employing GPE of PVDF/P(ViPrIm$^+$I$^-$) (4:6 m/m) gained the best properties with the open-circuit voltage of 0.694V and the short-circuit current of 12.752 mA. The formation of I_3^- plays an important role in the redox reactions between I^- and I_3^- contributed to the charge transfer process in DSSCs [33, 34]. P(ViPrIm$^+$I$^-$) as a single-ion conductor, in which iodide ion can migrate and imidazolium cation is immobilized, provides more I_3^- as the source of redox species when iodine is added. The superiority in transport of anionic species in the cell resulted in better photovoltaic performances.

4. Conclusions

P(ViPrIm$^+$I$^-$) as the polymeric ionic liquid was synthesized. A gel polymer electrolyte based on PVDF/P(ViPrIm$^+$I$^-$) blend polymer were prepared by soaking a porous membrane in an organic electrolyte solution containing the I^-/I_3^- redox couple. The incorporation of P(ViPrIm$^+$I$^-$) component into the polymer matrix changed significantly the morphology. The best ionic conductivity and the apparent diffusion coefficient of triiodide of GPEs were observed in the membrane with the weight ratio of PVDF/P(ViPrIm$^+$I$^-$) 7/3 owing to highest porosity and electrolyte uptake. Furthermore P(ViPrIm$^+$I$^-$) serving as iodide ion source improved the apparent diffusion coefficient of triiodide when the weight ratio of PVDF/P(ViPrIm$^+$I$^-$) was 6/4. A dye-sensitized solar cell employing GPE of PVDF/P(ViPrIm$^+$I$^-$) (4:6 m/m) yielded an open-circuit voltage of 0.694 V, short-circuit current of 12.752 mAcm^{-2} and the conversion efficiency of 5.66% at 1 sun illumination. The optimization of many parameters for the electrode preparation and the cell assembling is under study and the further improvement of the photovoltaic performance is expected in the near future.

References

[1] M. Grätzel, Nature **414** , 338 (2001)

[2] M. K. Nazeeruddin, P. Pechy, T. Renouard, S. M. Zakeeruddin, M. Grätzel, J. Am.Chem. Soc.**123**, 1613 (2001).

[3] J. E. Benedetti et al. J. Power Sources. **195**, 1246 (2010).

[4] Zhipeng Huo, Changneng Zhang, Xiaqin Fanga, Molang Caia, Songyuan Dai, Kongjia Wang, J. Power Sources. doi:10.1016 / j.jpowsour. 2009.12.107.

[5] E. Stathatos, P. Lianos, A. S. Vuk, B. Orel, Adv. Funct. Mater. **14**, 45 (2004).

[6] J. Bandara, H. Weerasinghe, Sol. Energy Mater. Sol. Cells. **85**, 385 (2005)

[7] J. Xia, N. Masaki, M. Lira-Cantu, Y. Kim, K. Jiang, S. Yanagida, J. Am. Chem.Soc. **130**, 1258(2008)

[8] Yukyeong Kim, Yung-Eun Sung, Jiang-Bin Xia , Monica Lira-Cantu, Naruhiko Masaki, Shozo Yanagida, Journal of Photochemistry and Photobiology A: Chemistry **193**, 77 (2008).

[9] P. Wang, Q. Dai, S. M. Zakeeruddin, M. Forsyth, D. R. MacFarlane, M. Grätzel, J. Am. Chem. Soc. **126**, 13590 (2004).

[10] P. Wang, S. M. Zakeeruddin, R. H. Baker, M. Grätzel, Chem. Mater. **16**, 2694 (2004).

[11] Huei-Ru Jhong, David Shan-Hill Wong, Chi-Chao Wan, Yung-Yun Wang, Tzu-Chien Wei, Electrochemistry Communications. **11**, 209 (2009).

[12] Chengwu Shi, Qian Ge, Fang Zhou, Molang Cai, Xiaoran Wang a, Xiaqin Fang, Xu Pan, Solar Energy. **83**, 108 (2009).

[13] Dong-Wan Seo, Subrata Sarker, Narayan Chandra Deb Nath, et al., Electrochimica Acta. **55**, 1483 (2010).

[14] Lei Guo, Xu Pan, Changneng Zhang, et al., Solar Energy. **84**, 373 (2010).

[15] E. Stathatos, P. Lianos, A. S. Vuk, B. Orel, Adv. Funct. Mater. **14**, 45 (2004).

[16] Pramod K. Singh, Kang-Wook Kim, Nam-Gyu Park, Hee-Woo Rhee, Synthetic Metals **158**, 590 (2008).

[17] Po-Yen Chen, Chuan-Pei Lee, R. Vittal, Kuo-Chuan Ho, Journal of Power Sources **195**, 3933 (2010).

[18] M. Yoshizawa, H. Ogihara, H. Ohno, Polym. Adv. Technol. **13**, 589 (2002).

[19] R. Marcilla, J. Alberto Blazquez, J. Rodriguez, J.A. Pomposo, D. Mecerreyes, J. Polym. Sci. A: Polym. Chem. **42** , 208 (2004).

[20] R. Marcilla, J. Blazquez, R. Fernandez, H. Grande, J. A. Pomposo, D. Mecerreyes, Macromol. Chem. Phys. **206**, 299 (2005)

[21] R. Marcilla, F. Alcaide, H. Sardon, J.A. Pomposo, C. Pozo-Gonzalo, D. Mecerreyes, Electrochem. Commun. **8**, 482 (2006)

[22] Bo Yu, Feng Zhou, Chengwei Wang , Weimin Liu, European Polymer Journal **43**, 2699 (2007).

[23] E. Azaceta, et al., Electrochim. Acta. doi:10.1016/j.electacta.2009.01.058.

[24] Yanmin Wang, Solar Energy Materials & Solar Cells **93**, 1167 (2009).

[25] Chengwu Shi, Qian Ge, Shikui Han, Molang Cai, Songyuan Dai, Xiaqin Fang, Xu Pan, Solar Energy **82**, 385 (2008).

[26] Tao Hai-jun , Tao Jie , Wang Tao, Wang Ling , Qin Liang , Xu Lu-lu, Trans. Nonferrous Met. Soc. China, 11, 2005.

[27] Dar-Jong Lin, Chi-Lin Chang, Chih-Kang Lee, Liao-Ping Cheng.European Polymer Journal **42**, 2407 (2006).
[28] N. K. Chunga, Y. D. Kwonb, D. Kim, J. Power Sources **124**, 148 (2003).
[29] A. G. Kontos, M. Fardis, M. I. Prodromidis, T. Stergiopoulos, E. Chatzivasiloglou, G. Apavassiliouc, P. Falaras, Phys Chem Chem Phys **8**, 767 (2006).
[30] M. Gratzel, Prog. Photovolt. Res. Appl. **8**, 171 (2000).
[31] Y. Saito, H. Kataoka, E. Quartarone, P. Mustarelli, J. Phys. Chem. B **106**, 7200 (2002).
[32] Y. Saito, A. M. Stephan, H. Kataoka, Solid State Ionics **160**, 149 (2003).
[33] M. Grätzel, Chem. Lett. **34**, 8 (2005).
[34] W. Kubo, K. Murakoshi, T. Kitamura, S. Yoshida, M. Haruki, K. Hanabusa, H. Shirai, Y. Wada, S. Yanagida, J. Phys. Chem. B **105**, 12809 (2001).

---

[*] Corresponding author: taojie@nuaa.edu.cn